The application of inexpensive and synthetic simple electrocatalyst CuFe-MoC@NG in immunosensor

LiSha Mei[a], WenTang Zhao[a], MengMeng Zhang[a], Yiju Song[a], Jiashuai Liang[a], Yan Sun[a], SiYu Chen, Hongling Li[a*], Chenglin Hong[a*]

[a] *Key Laboratory for Green Processing of Chemical Engineering of Xinjiang Bingtuan, School of Chemistry and Chemical Engineering, Shihezi University, Shihezi, 832003, China*

[*] Corresponding authors

Chenglin Hong E-mail address: hcl_tea@shzu.edu.cn Fax: +86-0993-2057270

Hongling Li E-mail address: lhl_tea@shzu.edu.cn Tel/Fax: Fax: +86-18009930289.

1. Reagents and instruments

Ammonium thiomolybdate $(NH_4)_2MoS_4$, (3-aminopropyl) triethoxysilane (APTES), gold chloride tetrahydrate ($HAuCl_4 \cdot 4H_2O$), Copper nitrate Cu $(NO_3)_2 \cdot 3H_2O$ potassium ferricyanide $K_3[Fe(CN)_6]$, ammonium molybdate $(NH_4)_6Mo_7O_{24} \cdot 4H_2O$ and sodium acetate were supplied by Aladdin Reagent (ShaNhai, China). Bovine serum albumin (BSA) was purchased from Alfa Aesar (Tianjin, China). CEA antigens, alpha-fetoprotein (AFP) antigens, anti-CEA antibodies and anti-AFP antigens were offered from ZheNzhou Biocell Co, Ltd. Phosphate buffered saline (PBS, 0.1 M), The electrolyte of the electrochemical measurement process was doubled by mixiN a solution to NaH_2PO_4 and Na_2HPO_4. Other chemicals and solvents are of analytical grade and ready for use without further purification. Deionized water was used duriN all experiments.

The Electrochemical measurements were investigated on CHI760 Electrochemical work station (ShaNhai Chenhua Instruments Co, Ltd, China). The three-electrode system was used in all Measurements: a GCE (4 mm in diameter) as the workiN electrode, a platinum wire electrode as the counter electrode and a saturated calomel electrode (SCE) as the reference electrode. The scanniN electron microscopy (SEM, Zeiss Supra 55VP) and the transmission electron microscopy (TEM, JEM-1200EX) were used for surface morphology characterization. The energy dispersive spectroscopy (EDS, Zeiss Supra 55VP) and Fourier transform infrared spectroscopy (FTIR, Nicolet iS10, Thermo Fisher, America) was used for elemental analysis.

2. Comparison of different signal amplification strategies

In sandwich immunosensors, the sensitivity depends mainly on whether the label used has adequate electrocatalytic properties. For comparative electrocatalytic analysis, the synthesized CuFe PBAs, MoS_2/Au NPs, and CuFe-MoC@NG nanocomplexes were all modified with 12.0 μL of 2.0 mg/mL at the electrodes. The bare GCE (curve a) has no H_2O_2 catalytic activity (Figure S7A). When the GCE is modified with CuFe PBAs, the current response gradually increases. When modifying GCE with MoS_2 /Au NPs (curve c). CuFe-MoC@NG shows excellent electrocatalytic properties (curve e) for reducing H_2O_2, and its structure provides additional active sites and increased surface area.

To obtain CuFe-MoC@NG nanocomposites with good catalytic properties and dispersion, the ratio of CuFe PBAs to Mo^{6+}, PVP content, and calcination temperature were studied to synthesize the expected nanocomposite.

3.3.1 Effect of ratio of CuFe PBAs to Mo^{6+}on Catalytic Performance

To optimize the structural and electrocatalytic properties, a series of CuFe PBAs were mixed with Mo^{6+} in different proportions and calcined products were called CuFe-MoC@NG-0, CuFe-MoC@NG-1, CuFe-MoC@NG -2, and CuFe-MoC@NG-3, where 0, 1, 2, and 3 represent the mass ratio of the introduced $(NH_4)_6Mo_7O_{24}\cdot 4H_2O$ dopant precursor to CuFe PBAs, respectively. The electrocatalytic performance of the calcined product reaches the maximum when the addition ratio of Mo^{6+} is 2 (Figure S7B). When the ratio is further increased, the possible accumulation of calcined externals increases resistance to mass transfer that reduces the contact of the internal material with H_2O_2, including the electrocatalytic performance. We choose an optimal mass ratio of 2 for the subsequent condition optimization.

3.3.2 Effect of different PVP content on catalytic performance

To explore the effect of the amount of PVP added to the electrocatalytic performance, a series of different in-mass PVP and precursors were mixed. The catalytic properties were then explored according to the mass ratio of $(NH_4)_6Mo_7O_{24}\cdot 4H_2O$ doped precursor to CuFe PBA of 2. The following become CuFe-MoC-0@NG, CuFe-MoC-1@NG, and CuFe-MoC-2@NG, where 0, 1, and 2 indicate the mass of the introduced PVP, respectively. The response signal of catalytic H_2O_2 decreases with an increasing amount of PVP addition (Fig S7C). The contact between CuFe and H_2O_2 is hampered by the formation of a graphene-like carbon layer after calcination of PVP, which is optimal for the catalytic reduction of H_2O_2 when PVP content is 0, but the calcination of the metal without PVP leads to a material size that is too large for the attachment of antibody labels. Thus, we selected a PVP addition content of 1.

3.3.3 Effect of calcination temperature on Catalytic Performance

Calcination temperature is a factor that affects the electrocatalytic performance. Here we have investigated the catalytic performance plots of the calcined products for H_2O_2 at 700 °C, 800 °C and 900 °C. As shown Fig S7D, indicates the highest performance of catalysis at 800 °C.

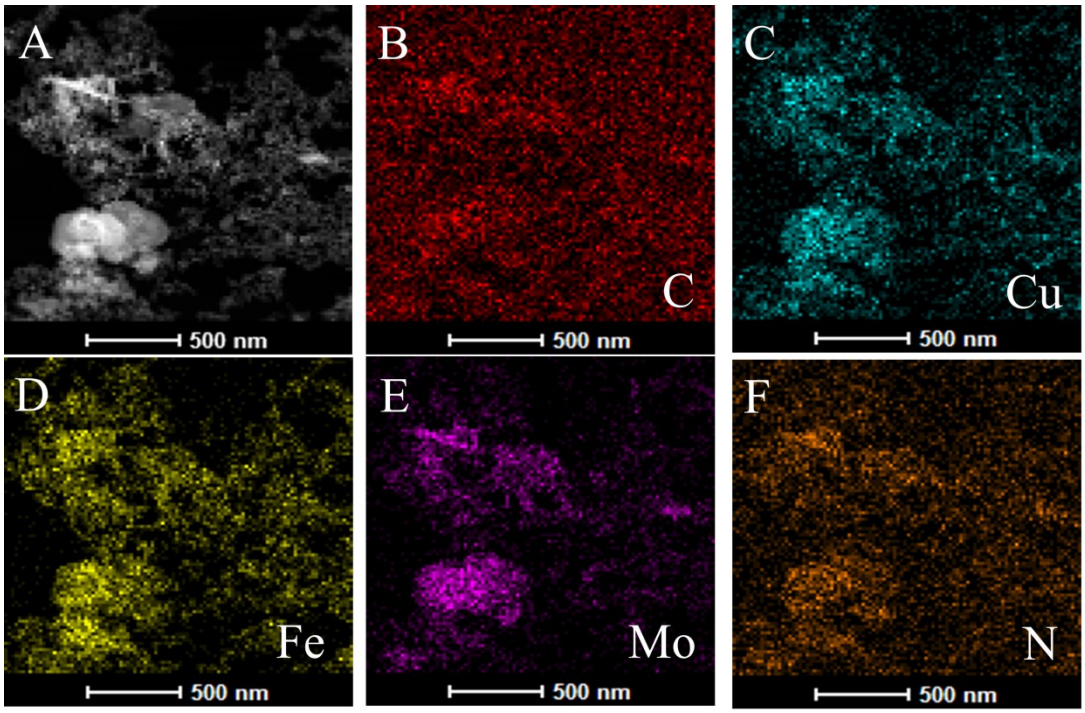

FigS1. Shows C, Cu, Fe, Mo and N elemental mapping of CuFe-MoC@NG.

3. Cyclic Voltammograms of CuFe-MoC@NG

In the proposed sandwich immunosensor, the signal amplification strategy mainly relies on CuFe-MoC@NG with high catalytic activity for H_2O_2 reduction. To investigate the electrocatalytic mechanism of CuFe-MoC@NG nanocomposites for H_2O_2 reduction, their electrocatalytic performance was further characterized by the cyclic voltammetry method. Figure S2 shows that the CV (curve a) of the CuFe-MoC@NG modified GCE before the addition of H_2O_2 does not show a significant reduction peak. After the addition of H_2O_2 (curve b), a sharp increase in y-reduction current was observed at -0.6 V, indicating that the CuFe-MoC@NG nanocomposites exhibit good electrocatalytic performance against H_2O_2.

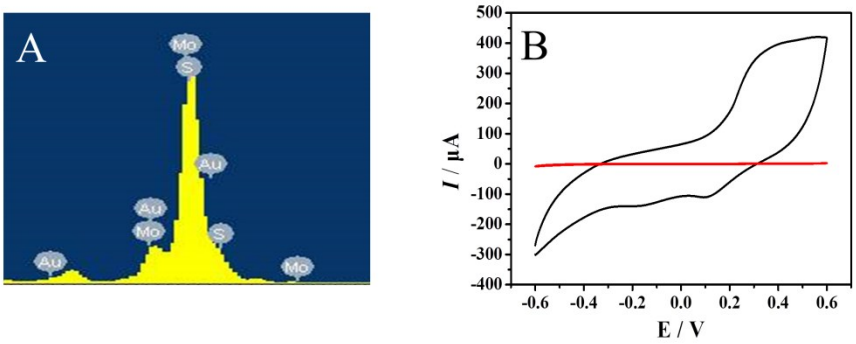

Fig S2 EDX (A) of MoS_2−Au nanocrystal, (B) CV experiments of CuFe-MoC@NG: (a) without H_2O_2; (b) with H_2O_2 (5mol/L).

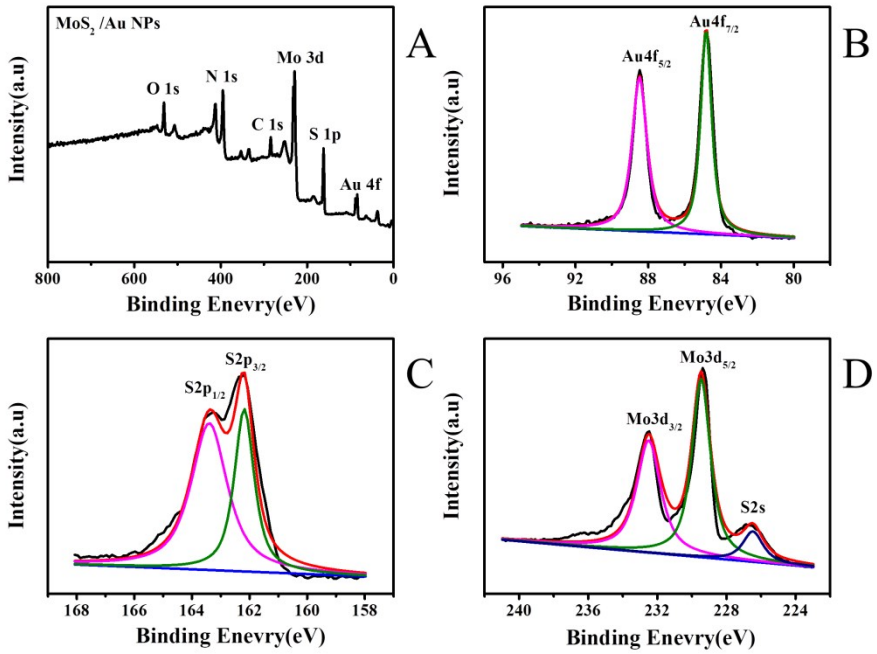

Fig.S3. XPS spectra for MoS_2/Au NPs nanohybrids: (A) survey, (B) Au, (C) S, (D) Mo.

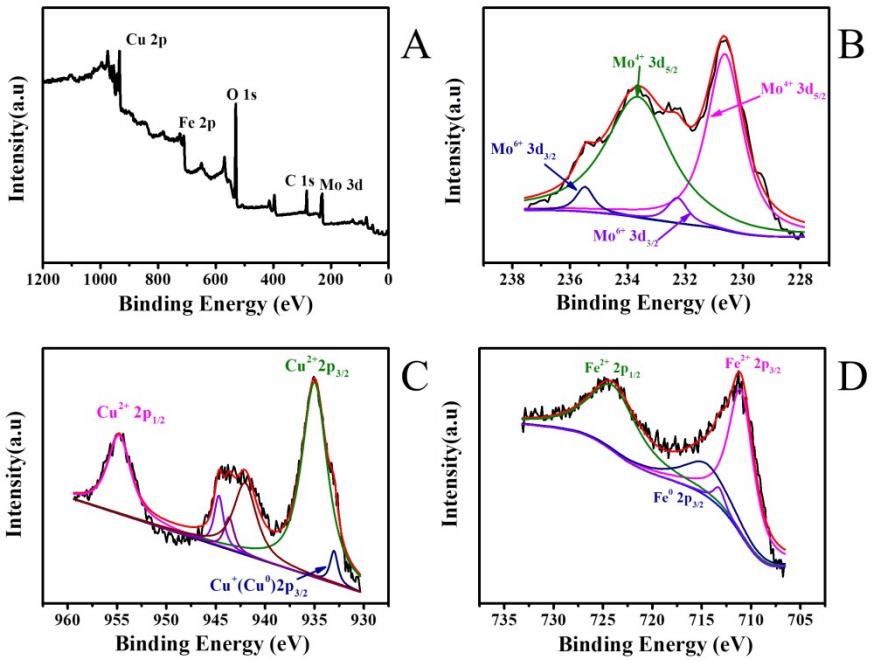

Fig.S4. XPS spectra for CuFe-MoC@NG nanohybrids: (A) survey, (B) Mo, (C) Cu, (D) Fe.

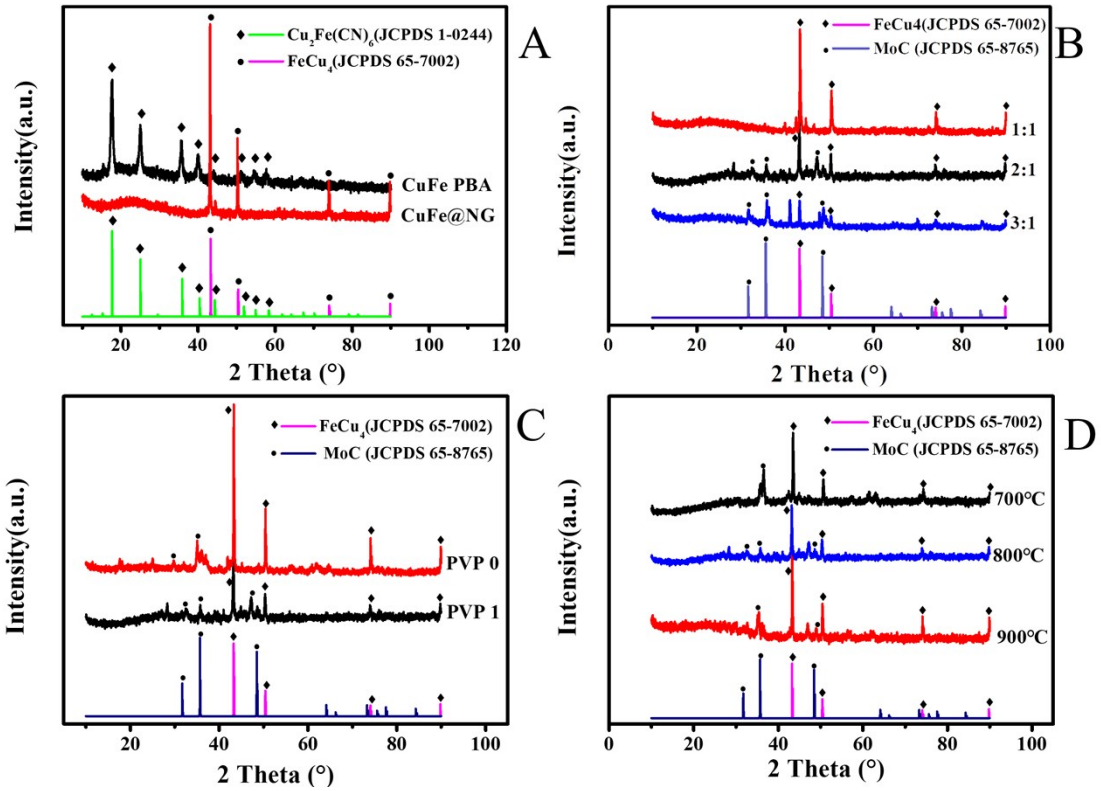

FigS5. (A) XRD spectra of CuFe PBA precursors and calcined samples, (B) XRD patterns of $(NH_4)_6Mo_7O_{24}\cdot 4H_2O$ and CuFe PBA precursors mixed at different ratios and calcined at 800 °C, (C) XRD spectra of $(NH_4)_6Mo_7O_{24}\cdot 4H_2O$ and CuFe PBA precursors (containing different amounts of PVP) after calcination at 800 °C, (D) XRD spectra of $(NH_4)_6Mo_7O_{24}\cdot 4H_2O$ with CuFe PBA precursors (2:1) after calcination at different temperatures.

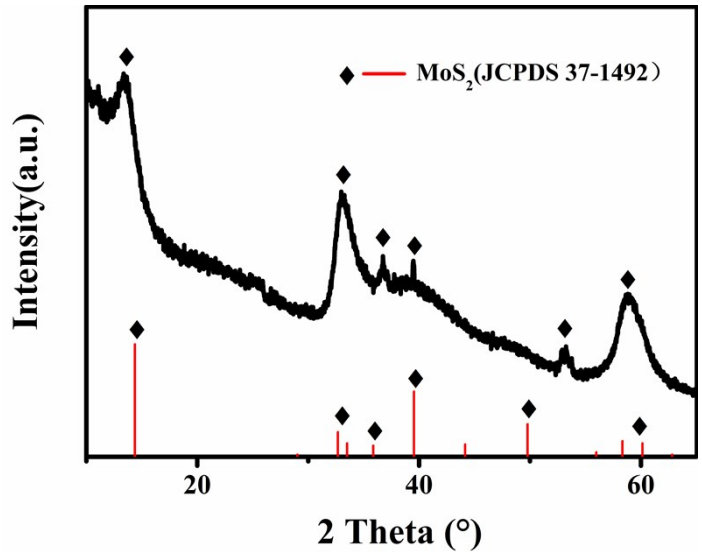

FigS6. (A) XRD spectra of MoS_2

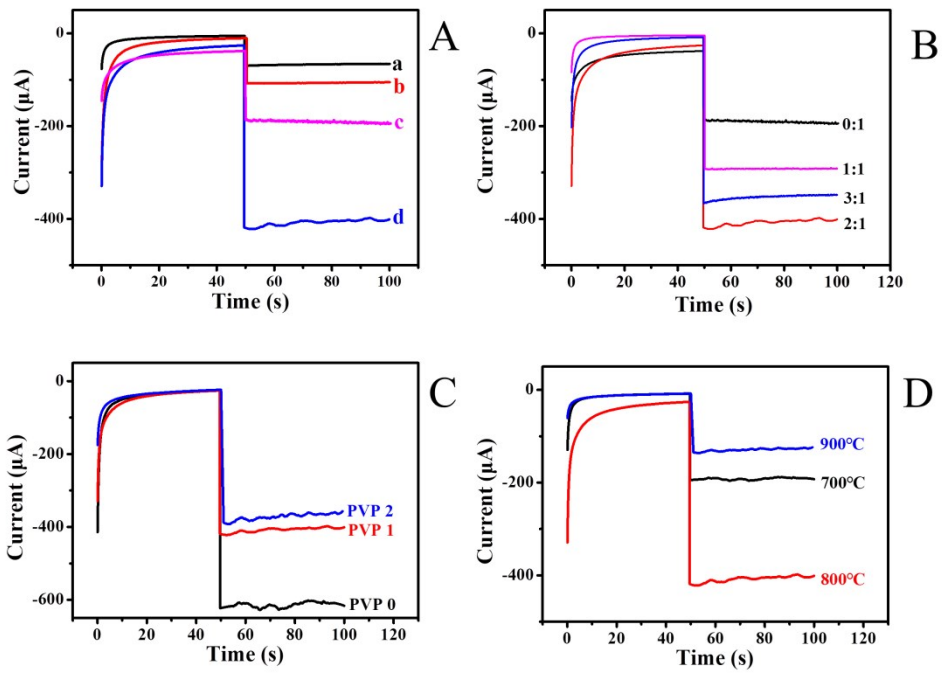

Fig.S7 (A) i–t of GCE/CuFe PBA (PVP=1) (a), GCE/MoS_2–Au NPs (b), GCE/CuFe@NG (PVP=1) (c) GCE/CuFe-MoC@NG(d); (B) Different ratios of Mo^{6+} and CuFe PBA; (C) Different PVP content; (D) Different calcination temperature.

Table S1 Assay results of clinical serum samples usiN this immunosensor and ELISA (n=3)

Samples	Method	Determined ($N\ mL^{-1}$)	Added ($N\ mL^{-1}$)	Total found ($N\ mL^{-1}$)	Recovery (%)	RSD (%)
Serum	Immunosensor[a]	3.20	0.10	3.23±0.07	98.5	2.2
			3.20	6.34±0.13	99.1	2.1
			5.0	8.39±0.19	102.7	2.3
			8.0	11.29±0.28	100.8	2.5
			10.0	13.61±0.41	103.6	3.0
	ELISA[a]	3.40	0.10	3.44±0.06	98.2	1.7
			3.20	6.55±0.14	99.2	2.1
			5.0	8.52±0.20	101.4	2.3
			8.0	11.64±0.33	102.1	2.8
			10.0	13.82±0.42	103.1	3.0

a: Mean value of three measurements.